Oncogene (2003) 22, 2993–3006

www.nature.com/onc

Genome-wide comparison of human keratinocyte and squamous cell carcinoma responses to UVB irradiation: implications for skin and epithelial cancer

Jean-Eudes Dazard[1], Hilah Gal[1,2], Ninette Amariglio[3], Gideon Rechavi[3], Eytan Domany[2] and David Givol*[,1]

[1]*Department of Molecular Cell Biology, Weizmann Institute of Science, Rehovot 76100, Israel;* [2]*Department of Physics of Complex Systems, Weizmann Institute of Science, Rehovot 76100, Israel;* [3]*Department of Pediatric Hemato-Oncology and Functional Genomics, The Chaim Sheba Medical Center and Sackler School of Medicine, Tel-Aviv University, Israel*

To gain insight into the transformation of epidermal cells into squamous carcinoma cells (SCC), we compared the response to ultraviolet B radiation (UVB) of normal human epidermal keratinocytes (NHEK) versus their transformed counterpart, SCC, using biological and molecular profiling. DNA microarray analyses (Affymetrix®, ~12 000 genes) indicated that the major group of upregulated genes in keratinocytes fall into three categories: (i) antiapoptotic and cell survival factors, including chemokines of the CXC/CC subfamilies (e.g. *IL-8*, *GRO-1*, *-2*, *-3*, *SCYA20*), growth factors (e.g. *HB-EGF*, *CTGF*, *INSL-4*), and proinflammatory mediators (e.g. *COX-2*, *S100A9*), (ii) DNA repair-related genes (e.g. *GADD45*, *ERCC*, *BTG-1*, *Histones*), and (iii) ECM proteases (*MMP-1*, *-10*). The major downregulated genes are *ΔNp63* and *PUMILIO*, two potential markers for the maintenance of keratinocyte stem cells. NHEK were found to be more resistant than SCC to UVB-induced apoptosis and this resistance was mainly because of the protection from cell death by secreted survival factors, since it can be transferred from NHEK to SCC cultures by the conditioned medium. Whereas the response of keratinocytes to UVB involved regulation of key checkpoint genes (*p53*, *MDM2*, $p21^{Cip1}$, *ΔNp63*), as well as antiapoptotic and DNA repair-related genes – no or little regulation of these genes was observed in SCC. The effect of UVB on NHEK and SCC resulted in upregulation of 251 and 127 genes, respectively, and downregulation of 322 genes in NHEK and 117 genes in SCC. To further analyse these changes, we used a novel unsupervised coupled two-way clustering method that allowed the identification of groups of genes that clearly partitioned keratinocytes from SCC, including a group of genes whose constitutive expression levels were similar before UVB. This allowed the identification of discriminating genes not otherwise revealed by simple static comparison in the absence of UVB irradiation. The implication of the changes in gene profile in keratinocytes for epithelial cancer is discussed.
Oncogene (2003) **22,** 2993–3006. doi:10.1038/sj.onc.1206537

*Correspondence: D Givol; E-mail: david.givol@weizmann.ac.il
Received 17 December 2002; revised 21 February 2003; accepted 24 February 2003

Keywords: microarray; clustering; epidermis; apoptosis; chemokines

Introduction

Skin is the largest organ in the body, whose outermost adult tissue is the epidermis. The epidermis is the stratified squamous epithelium composed primarily of keratinocytes and a few melanocytes. As the primary interface between the environment and the body, it has developed several defense mechanisms including protection against the harmful effects of solar ultraviolet (UV) radiation. Ultraviolet B (UVB) radiations (280–320 nm) are the most energetic and DNA damaging rays of the UV solar spectrum that reach the surface of the earth (Cleaver and Crowley, 2002). The skin is the site of a large variety of malignant neoplasms, but basal cell carcinoma (BCC) and squamous cell carcinoma (SCC), both derived from keratinocyte transformation, and melanomas, derived from melanocytes are by far the most frequent types of skin cancers. Incidence of human skin cancer has increased considerably worldwide over the last few decades (Gloster and Brodland, 1996) and exposure to UV radiation has been found to be the major etiological factor leading to the precancerous stage of actinic keratosis (AK) and to the induction and development of skin cancers (Soehnge *et al*., 1997; Armstrong and Kricker, 2001). Although BCC and SCC account for less than 0.1% of patient deaths because of cancer, they are the most common of all human malignancies (Cleaver and Crowley, 2002) and can serve as useful models for the development of other epithelial cancers.

The UV-induced skin carcinogenesis has been modelled as a multistage process: a UV-specific mutagenic event of a target gene (initiation) is followed by clonal expansion of damaged cells (promotion), progression into precancerous state and eventually to uncontrolled proliferation and invasion (Brash, 1997). However, potent antitumorigenic mechanisms are believed to act in opposition to the emergence of mutational events. Cancers prevail only when these mechanisms have failed (Evan and Vousden, 2001). In the epidermis, the prevention of cancer progression is thought to be mediated through correction

of the mutations or, alternatively, elimination of the damaged cells by driving them toward apoptosis, senescence, or terminal differentiation. In this study, we describe the effects of UVB radiation on the gene expression profile of normal and transformed keratinocytes. Since we applied biologically relevant carcinogenic radiations to the appropriate target cell type, our *in vitro* results are relevant to the risk assessment in the carcinogenic process *in vivo*. Normal human epidermal keratinocytes (NHEK) were found to be more resistant than SCC to UVB-induced apoptosis, and this resistance is mainly because of the protection from cell death by secreted survival factors, which can be transferred from NHEK to SCC cultures. The evasion of apoptosis by keratinocytes in a DNA damaging context may potentially lead to undesirable effects by permitting the survival of residual mutant cells that accumulate mutations and may be the seeds for future cancer development.

Global analysis of gene expression by means of microarrays has become an important tool to study a broad range of complex problems, in particular in cancer biology. Although recent studies have begun to explore genes whose expression in keratinocytes is regulated by low doses of UVB (Li *et al*., 2001; Sesto *et al*., 2002), many of the molecular events associated with transformation and metastatic tumor progression in human SCC remain unknown. In an attempt to gain insight into the transformation events associated with SCC, we used DNA microarrays and an advanced unsupervised clustering method, coupled two-way clustering (CTWC) (Getz *et al*., 2000), to compare the differential gene expression profiles of the two cell types, assuming that normal keratinocytes should differ from their tumoral counterparts not only in their constitutive (static) gene expression profiles, but also in their (dynamic) response to an oncogenic stimuli (UVB irradiation). We show that the major group of upregulated genes in keratinocytes are (i) chemokines of the CXC/CC subfamilies (e.g. *IL-8*, *GRO-1*, *-2*, *-3*, *SCYA20*), growth factors (e.g. *HB-EGF*, CTGF, *Insulin-like 4*), and proinflammatory mediators (e.g. *COX-2*, *S100A9*), also known as antiapoptotic and cell survival genes, (ii) DNA repair-related genes (e.g. *GADD45*, *ERCC*, *BTG-1*, *Histones*), and (iii) ECM proteases (*MMP-1*, *-10*). The major downregulated genes include *ΔNp63* and *PUMILIO*, two potential markers for the maintenance of stem cells. Whereas the response of keratinocytes to UVB involved regulation of key checkpoint (*p53*, *MDM2*, *p21^{Cip1}*, *ΔNp63*), antiapoptotic and DNA repair-related genes (see above), little or no regulation of these genes is observed in SCC. The implication of the changes in gene expression in keratinocytes for SCC and epithelial cancer in general is discussed.

Results and discussion

Time- and dose-dependent response of normal keratinocytes to UVB irradiation

We first assessed the effects of a single UVB exposure on normal keratinocytes (NHEK), on the basis of survival curves, cellular morphology, cell cycle analysis, and protein expression criteria. At the highest doses tested (800 J/m^2), the proportion of surviving cells was 70%, and more than 84% of cells were alive at 400 J/m^2, as observed 24 h following irradiation (Figure 1a). Cellular morphology of NHEK (Figure 1b) and sub-G1 DNA content analysis (Figure 1c) confirmed that virtually all keratinocytes irradiated at 200 J/m^2 survive the UVB exposure. FACS analyses revealed no evident cell cycle arrest in NHEK at the UVB doses applied (Figure 1c). The time- and dose-dependent response of keratinocyte to UVB irradiation is well illustrated by the correlation of the level of cell death during 6–24 h postirradiation with the dose range of 200–800 J/m^2 (Figures 1a–c). A similar correlation was found for the expression of ΔNp63, which is gradually downregulated between 6 and 24 h following irradiation or between doses of 200 and 800 J/m^2 (Figure 1d). We chose a UVB dose of 400 J/m^2 as the representative dose to analyse the overall molecular radiation response in keratinocytes. This dose is similar to the estimated UVB dose received in a single or chronic sunburn (Selgrade *et al*., 2001; Hanson and Clegg, 2002).

Normal keratinocytes are more resistant than SCC cells to UVB-induced apoptosis

NHEK, when irradiated with a single dose of 400 J/m^2 UVB, showed greater resistance to apoptosis than SCC12B2 (Figure 2a, top): 2–3-fold more SCC12B2 cells initiated apoptosis at any given time point following irradiation (Figure 2b left). This difference is even more pronounced (5–6-fold) when multiple low UVB doses (200 J/m^2) were applied (Figures 2a down, 2b right). We also compared the protein expression levels of some apoptotic markers after a single 400 J/m^2 irradiation. Activation of caspase-8, -9, and -3 along with their substrate proteolysis such as PARP are hallmarks of the mammalian apoptotic pathway (Green and Evan, 2002). A remarkable difference between SCC and NHEK was noticed, in particular for caspase-9 and PARP activation. SCC12B2 cells showed significant activation of these markers between 6 and 12 h postirradiation, whereas in NHEK, activation of these genes was barely detectable (Figure 2c). Taken together, these data are consistent with the higher resistance to apoptosis of NHEK as compared to SCC12B2 cells.

Differential effects of UVB irradiation on ΔNp63, p53, p16^{Ink4a}, and p53-regulated genes between NHEK and SCC

Kinetics of ΔNp63, p53, and p16^{Ink4a} expression and expression of typical p53 target genes, for example, *p21^{Cip1}*, and *MDM2*, were also compared at the protein level between NHEK and SCC12B2 cells after a single UVB dose of 400 J/m^2. Despite the absence of regulation at the transcriptional level (our DNA chip results and (Li *et al*., 2001)), the p53 protein is rapidly stabilized after irradiation (3 h), as expected in response to a cellular stress (Michael and Oren, 2002), and is able to

a

	0 J/m²	100 J/m²	200 J/m²	400 J/m²	800 J/m²
0h	99.2	99.2	99.2	99.2	99.2
6h	99.2	99.1	98.0	96.6	91.7
12h	99.2	97.0	94.6	92.4	84.8
24h	99.2	96.5	93.0	84.3	70.5

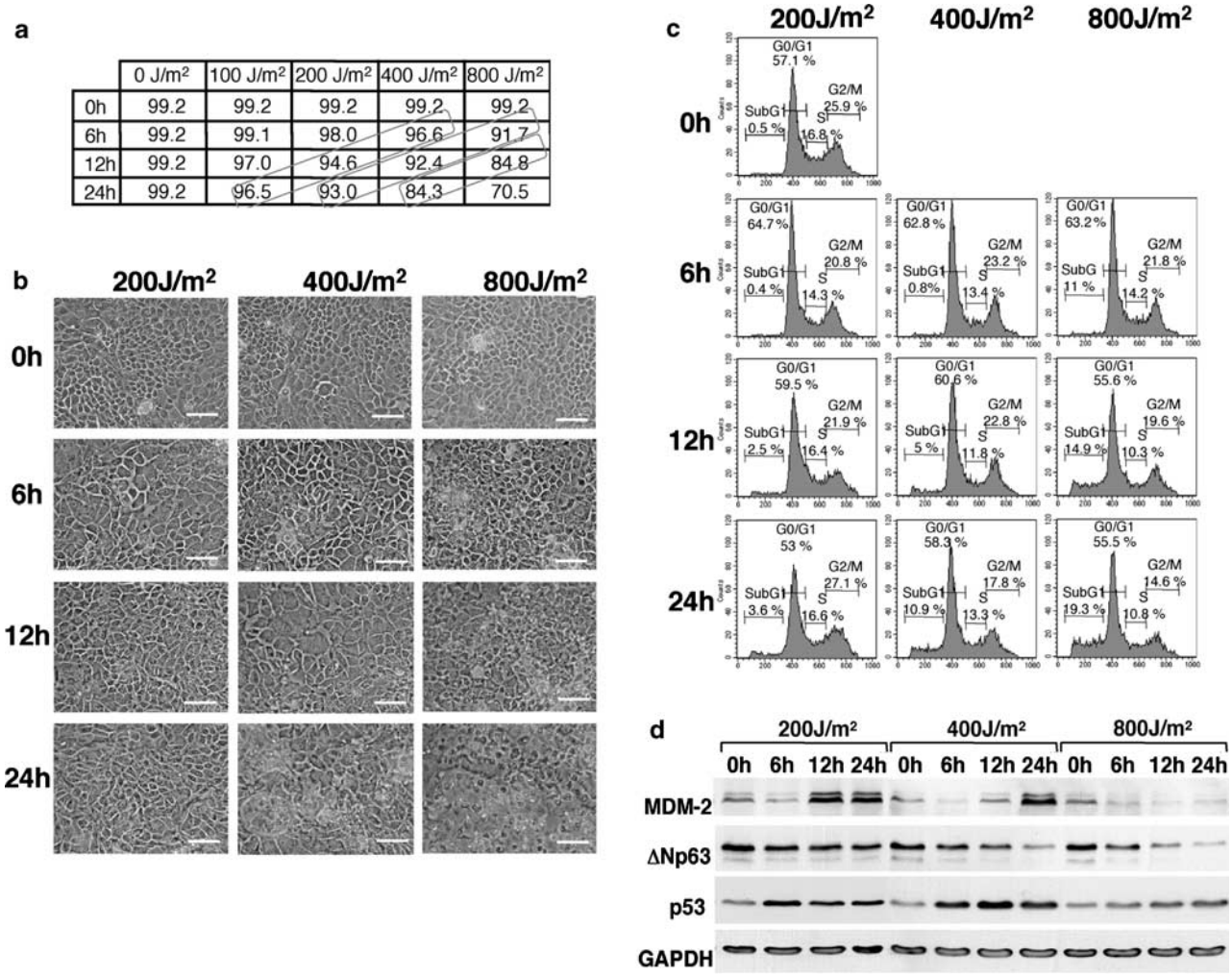

Figure 1 Dose- and time-dependent effects of a single UVB irradiation on normal keratinocytes (NHEK). UVB irradiation (200, 400, or 800 J/m²) was applied once to NHEK cells, and assessed 6, 12, and 24 h postirradiation. (**a**) Effect of UVB irradiation on cell viability as determined by trypan blue uptake assay. Similar time and dose responses are circled together. (**b**) Cell culture morphologies (bar = 50 μm). (**c**) Cell cycle analysis as determined by FACS histogram plots of DNA content. (**d**) Western blot analysis of MDM2, ΔNp63, and p53 protein expression. Uniform loading was confirmed by GAPDH internal control (50 μg/lane, 8% acrylamide gel)

transactivate its two typical target genes, *MDM2* (1.9-fold at 12 h) and $p21^{Cip1}$ (fivefold at 24 h) (category 1, Table 1). We do not see significant increase in $p16^{Ink4a}$ RNA levels (Chazal *et al*., 2002), but there is an accumulation of the protein as early as 3 h and until 48 h postirradiation (Figure 2d). This pattern of expression parallels that of p53 and supports the paradigm that these two tumor suppressors are involved in the protective response to UVB and in the prevention of the progression from benign AK to SCC (Ziegler *et al*., 1994; Soufir *et al*., 1999). The *p63* gene, a recently identified member of the p53 family, plays an essential role during mammalian development of epithelial tissues, including stratified squamous epithelia like the epidermis (Yang *et al*., 1999); however, in contrast to p53, this gene does not appear to be targeted by mutations in cancer. In keratinocytes, products of the *p63* gene were found to be potential markers of progenitors or the so-called adult 'stem cells' (Parsa *et al*., 1999; Pellegrini *et al*., 2001). Furthermore, products of the *p63* gene in keratinocytes, namely the ΔNp63 α, β, γ isoforms, were shown to act as p53 dominant-negative partners (Yang *et al*., 1998), able to counteract p53-dependent apoptosis *in vivo* (Liefer *et al*., 2000). Upon UVB irradiation, we observed a downregulation of these forms especially as of 24 h postirradiation, and a concomitant induction of the p53-target genes $p21^{Cip1}$ and *MDM2* (Figures 1d, 2d), suggesting that the p53 transcriptional activity required for UVB-induced apoptosis may also be released at this time. Therefore, ΔNp63 may have an important role in the regulation of the response to UVB irradiation, as well.

In sharp contrast to NHEK, no regulation of the above genes was found in SCC12B2 cells (Figure 2d). It is of interest that p53 (mutated in SCC; Burns *et al*., 1993) as well as $p21^{Cip1}$ show high expression at 0 h, and ΔNp63 remains at high level even at 48 h in SCC12B2 (Figure 2d). The total lack of regulation of these genes in SCC12B2 in response to UVB may reflect part of their transformed state.

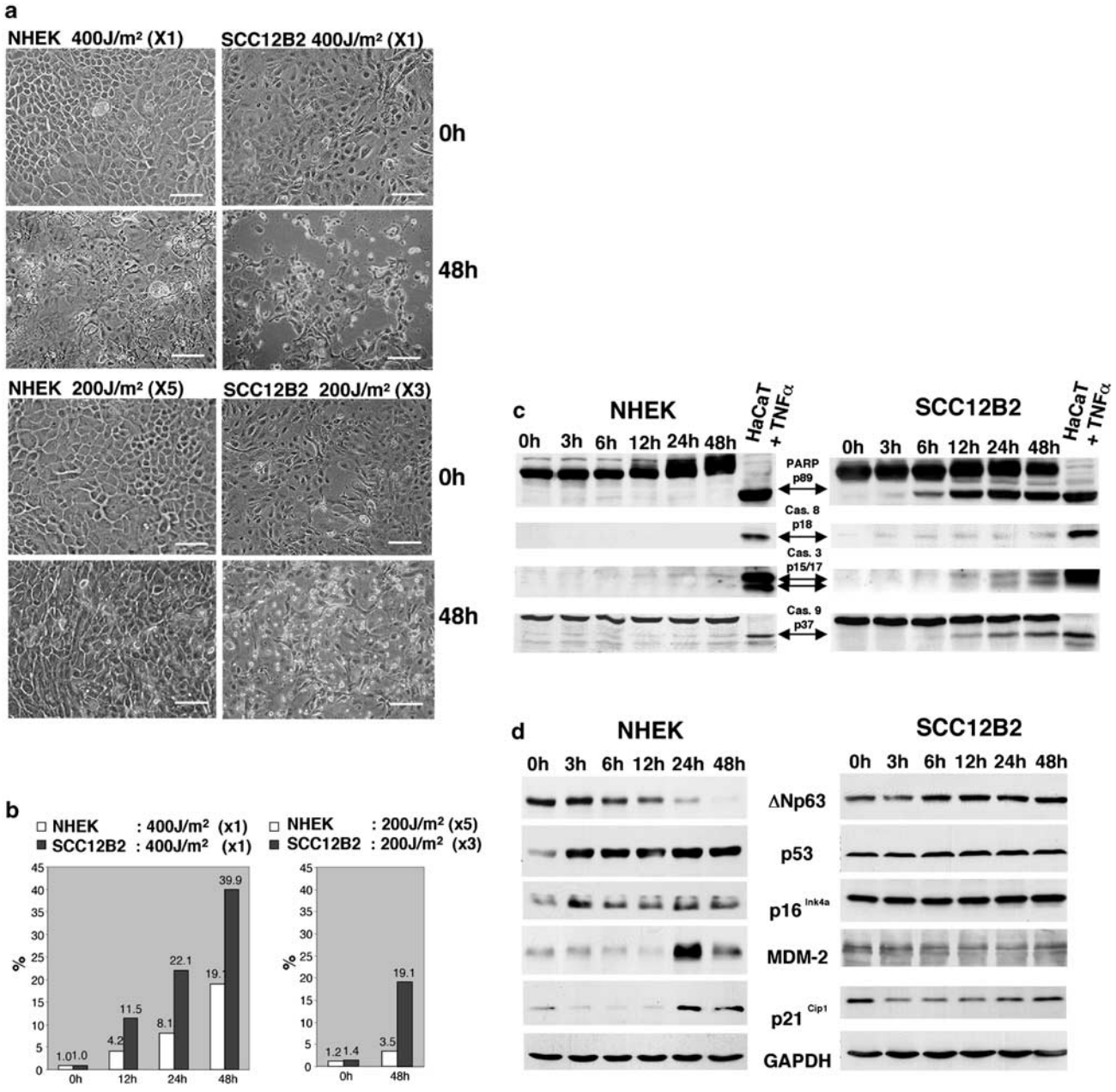

Figure 2 Effects of a single (400 J/m²) or multiple (200 J/m²) doses of UVB irradiation on NHEK and SCC12B2. (**a**) Cell culture morphologies (bar = 50 μm), before (0 h) and after UVB irradiation (48 h). Upper panel: single irradiation ($\times$ 1), lower panel: multiple irradiations ($\times$ 3 or $\times$ 5). (**b**) Percent (%) of sub-G1 DNA content 48 h after a single (left side), or multiple (right side) UVB irradiations. Empty bars: NHEK, shaded bars: SCC12B2. (**c**) Western blot analysis of PARP and caspase cleavage. Both full-length and cleaved forms (p89) of PARP are shown. For caspases, only the low MW active forms of caspase-8 (p18), caspase-3 (p15/17 doublet), and caspase-9 (p37) are shown. TNFα-treated HaCaT (lanes 7 and 14) served as a positive control marking the MW of cleaved forms (arrows) subsequent to full cleavage in these cells (50 μg/lane, 15% acrylamide gel). (**d**) Western blot analysis of protein expression of cornifin, an epidermal terminal differentiation marker and of proliferation-related genes (ΔNp63, p53, $p16^{Ink4a}$, MDM-2, $p21^{Cip1}$). GAPDH was used as an internal control (50 μg/lane, 8% acrylamide gel)

UVB-induced conditioned medium from NHEK can transfer protection from apoptosis

To further investigate why normal keratinocytes undergo substantially less apoptosis than their tumor counterparts, we tested whether this protection resulted from the presence of factors secreted into the media. When the culture medium of NHEK cultures was replaced with fresh medium every 6 h following irradiation at 400 J/m², the resistance to apoptosis was reduced: a partial cleavage of PARP was detected and the sub-G1 DNA content was 19% as compared to 6% without change of medium (lanes 1 and 2, Figure 3a). However, when the same protocol was applied to SCC12B2 cells in

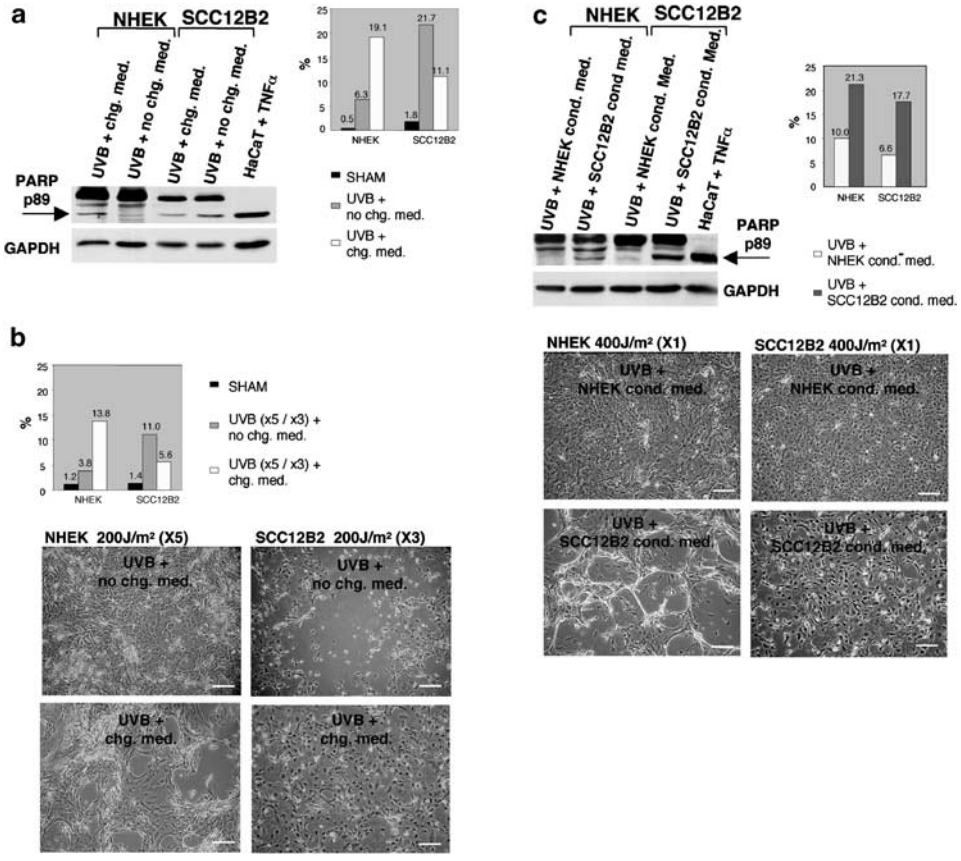

Figure 3 Effect of change of medium and of medium exchange between NHEK and SCC12B2 cells, after UVB irradiation. (**a**) Western blot analysis of PARP cleavage and sub-G1 DNA content 24 h following a single UVB irradiation (400 J/m^2). NHEK (lanes 1 and 2) and SCC12B2 (lanes 3 and 4) with change of medium (lanes 1 and 3) or without (lanes 2 and 4). Sub-g1 DNA content in NHEK (left side) and SCC12B2 (right side). (**b**) Cell culture morphologies (bar = 50 μm) and sub-G1 DNA content 48 h following multiple UVB irradiation (200 J/m^2 $\times$ 5 or $\times$ 3). NHEK (left side pictures) and SCC12B2 (right side pictures) with change of medium (bottom pictures) or without (top pictures). Percent (%) of sub-G1 DNA content in NHEK (left side) and SCC12B2 (right side). (**c**) Effect of exchange of UV-conditioned medium on cell death. Western blot analysis of PARP cleavage percent (%) of sub-G1 DNA content and cell morphology (bar = 50 μm, bottom panel) 48 h following a single UVB irradiation (400 J/m^2). Upper panel: NHEK maintained in conditioned medium from NHEK (lane 1) or SCC12B2 (lane 2), SCC12B2 cells maintained in conditioned medium from NHEK (lane 3) or SCC12B2 (lane 4). TNFα-treated HaCaT (lane 5), positive control shown in parallel as described above

culture, an inverse effect was observed, reflected by decreased sub-G1 DNA population (11% as compared to 21%) and reduced cleavage of PARP (lanes 3 and 4, Figure 3a). This effect was also reproducible at multiple daily UVB doses of 200 J/m^2 (5 days for NHEK and 3 days for SCC12B2), although noticeably less apoptosis was observed overall in both cell types subjected to fractionated UVB irradiation (Figure 3b; compare also Figure 2b left to right). The morphology of the cell cultures also confirmed these observations (Figure 3b). Finally, to test whether the protection from apoptosis, or conversely the enhancement of apoptosis, could be transferred by the media, we switched the conditioned media from the two UV-irradiated cell cultures (NHEK or SCC12B2) upon renewing the culture medium. PARP cleavage in SCC12B2 cells is barely detectable when they were maintained in conditioned media from NHEK cells in contrast to the marked cleavage of PARP when they were exposed to their own conditioned media (lanes 3 and 4, Figure 3c). On the other hand, there is an elevation of PARP cleavage in NHEK cells when exposed to conditioned medium from SCC12B2 (lanes 1 and 2, Figure 3c). In line with these molecular changes, the sub-G1 DNA content of cells and morphology of the cells also confirm the enhancement or protection from apoptosis in the cell cultures (Figure 3c). These results indicate that the UVB-induced conditioned medium from NHEK cells can transfer the protection from apoptosis to SCC12B2 cells, and conversely, the UVB-induced medium from SCC12B2 can sensitize NHEK cells to apoptosis.

DNA repair and apoptosis control are the major responses in the transcriptional program of normal keratinocytes to UVB irradiation

In an attempt to gain insight into changes in gene expression resulting from UVB, we performed DNA microarray analysis on RNA derived from cultures treated with UVB. We applied an arbitrary filter level of twofold change in the ratios of gene expression in at least two time points to identify UVB-modulated genes

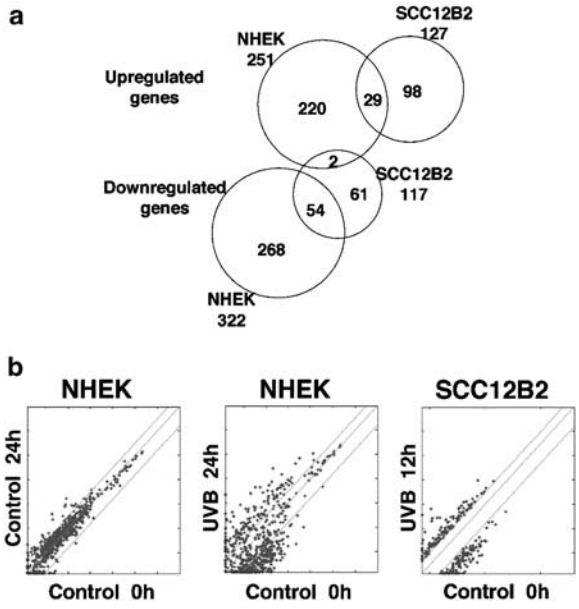

Figure 4 Change of gene expression in NHEK and SCC12B2 cells following a single dose (400 J/m^2) of UVB irradiation. (**a**) Venn diagram showing the number of up and downregulated genes in NHEK and SCC using a filter of twofold up- and threefold downregulation in at least two time points. (**b**) Scatter plot of changes of expression of monitored genes in NHEK and SCC cells. Left panel: changes of gene expression in NHEK between sham-irradiated controls. Middle panel: changes of gene expression in NHEK between control 0 h (sham irradiated) and 24 h following UVB irradiation. Right panel: changes of gene expression in SCC12B2 between control 0 h (sham irradiated) and 12 h post UVB irradiation

(Kannan *et al*., 2001). As a result, we came up with a list of 251 upregulated and 788 downregulated genes, representing approximately 18% of the 'legal' genes (approximately ~1.5–2% of the human genome) and 10-fold more than that reported for a single transcription factor, for example, p53 (1.8% of genes; Zhao *et al*., 2000). For practical reasons, we downsized the downregulated list to those that showed a threefold change of expression and ended up with a list of 322 UV-regulated genes in NHEK (Figure 4a). Similarly, a list of 127 upregulated and 117 downregulated genes was drawn for SCC cells (Figure 4a). Table 1 depicts selected genes of interest as they appear in the full lists (Tables 2 and 3, online supplemental data). Scatter plot of changes of expression of the genes modulated in NHEK (573) and SCC (244) confirmed the choice of the thresholds used, since in control cells, gene expression remained contained between the twofold and threefold borderlines when measured in the absence of UVB irradiation at 0 and 24 h (Figure 4b). UVB irradiation rapidly induces two predominant types of specific DNA damage, namely pyrimidine dimers and [6–4] pyrimidine-pyrimidinone photoproducts (Pfeiffer, 1997). These lesions induce upregulation of DNA repair genes, mainly from the nucleotide excision repair (NER) machinery (Sage *et al*., 1996). In our list, several genes related to DNA repair are upregulated, including, the endonuclease *ERCC1*, the helicase *ERCC2*, and the pleiotropic genes *GADD45A*, *GADD45B*, *TOB1*, and *BTG1* (category 3, Table 1). Interestingly, numerous histones, including H1, H2A isoforms, and H2B are also upregulated (category 12, Table 1). Recently, Martini *et al*. (2002) suggested a specific role of histone H2B in UV-induced DNA repair processes in yeast, and cells from mice lacking *H2AX* exhibit impaired recruitment of specific DNA repair complexes to IR-induced nuclear foci (Bassing *et al*., 2002; Celeste *et al*., 2002). Therefore histones appear to be critical for facilitating the assembly of specific DNA-repair complexes on damaged DNA, although how an increase in specific histone synthesis may support this process is still not understood. Altogether, these effects indicate the important role of DNA repair in UV-induced carcinogenesis, since unrepaired UV-induced lesions will result in mutagenesis, and the amount of unrepaired lesions depends on the interplay between the repair rate and the time available for DNA repair within the cell cycle (Greinert *et al*., 2000). Further evidence for the importance of DNA repair processes in the induction of skin cancer stems from the DNA repair disorders Xeroderma Pigmentosum (XP), Cokayne Syndrome (CS), and Trichothiodystrophy (TTD) (Cleaver and Crowley, 2002).

DNA damage signals to both DNA repair and apoptotic systems. Our results show that UVB simultaneously induces the expression of several pro and antiapoptotic genes in keratinocytes (category 2, Table 1). However, apart from the proapoptotic genes *CRADD*, *TSSC3*, and *APR* (*NOXA*), other notable proapoptotic genes, for example, *TNF*α, *BAX*, *BAK*, *BID*, and *PUMA* remained unchanged (category 2, Table 1). In contrast, there is a sustained (*ΔNp63*) or increased (*BCL-2*, *TNFAIP3*, *IER3*, *API5L1*) expression of antiapoptotic genes (categories 9, 2, Table 1). Moreover, two heat shock proteins (*HSP70* and *HSP90*) are also induced as early as 0.5 h (category 2, Table 1) following irradiation. These *HSPs* are inducible by UVB irradiation in NHEK *in vivo*, and are known to protect cells from apoptosis induced by various stimuli including UVB. In addition, the downregulation of *c-Myc* and *E2F* can be considered antiapoptotic (category 11, Table 1).

In addition to the above genes, keratinocytes also express upon UVB stress a wide variety of cytokines and secreted factors. Particularly noticeable is the marked upregulation of chemokines of the CXC/CC subfamilies (*IL-8* (>71-fold), *SCYA20* (21-fold), *GRO-1* (3.2-fold), *GRO-2* (sixfold), *GRO-3* (7.9-fold)), as well as *HB-EGF* (~10-fold), *IL-6* (3.7-fold), *CTGF* (9.3-fold), *CYR61* (3.6-fold), and *INSL4* (26-fold) a growth factor of the IGF family (category 6, Table 1). These secreted factors support cell growth and are known as survival factors (Lotem *et al*., 1999), which is consistent with the protective effect of the conditioned medium against UVB-induced apoptosis reported in this study (Figure 3). Of note, 10 out of the 14 upregulated genes in category 6 have a role in inflammation (labeled '+' in category 6, Table 1). Besides the aforementioned chemokines, these include the cyclooxygenase *COX-2* (24-fold) and *S100A9* (sixfold). Consistent with these findings, upon

UVB stress, keratinocytes are known to produce numerous cytokines and inflammatory mediators involved in acute phase and immunologic reactions (Garssen and van Loveren, 2001). In the UV inflammatory signaling pathway, IL-1β, TNFα, and reactive oxygen species (ROS) are induced. In response to these specific inflammatory stimuli, the transcription factors NF-*k*B, JunD/c-*fos*, and p53 are subsequently activated (Chung *et al*., 2001; Xie, 2001). In turn, NF-*k*B induces target genes such as *IL-1*, *IL-6*, *IL-8*, *GRO-1*, *TNF*α, *COX-2* (Loukinova *et al*., 2001; Xie, 2001; Karin *et al*., 2002). Similarly, p53 transactivates *HB-EGF* a newly discovered p53-target gene protecting cells against H2O2-induced apoptosis (Fang *et al*., 2001). Furthermore, COX-2 expression was recently shown to result from the p53-mediated activation of the HB-EGF->Ras/Raf/MAPK->COX-2 pathway, thereby counteracting p53- or genotoxic stress-induced apoptosis (Han *et al*., 2002). Other studies have shown that COX-2 itself is in the survival pathway of NF-*k*B (Brune and von Knethen, 2002) and contributes significantly to the tumorigenic potential of epithelial cells by increasing adhesion to ECM and inducing the expression of the survival genes *BCL-2* (3.6-fold, Table 1) and *AKT* (Tsujii and DuBois, 1995).

Collectively, our results provide indications of a protective response in normal keratinocytes against apoptosis, consistent with the relative resistance to cell death described in NHEK cells (Figures 1–3). Clearly, the balance between the pro- and antiapoptotic genes determines the cell fate, and this is probably linked to the success of DNA damage repair. In support of this notion, Decraene *et al*. (2002) recently proposed that in normal keratinocytes the onset of UVB-induced apoptosis following UVB irradiation is delayed by specific growth factors, providing more time for the repair of UV-specific DNA damage.

UVB irradiation also increased the levels of *ornithine decarboxylase* (*ODCI*) (3.5-fold, category 1, Table 1), another stress-related protein, which plays an important role in both normal cellular proliferation and growth of tumors, with a particular incidence in human skin photocarcinogenesis (Ahmad *et al*., 2001). In the inflammatory response, IL-8 was also shown to induce the release of matrix metalloproteinases (MMPs) from target inflammatory competent cells, thereby enabling vascular permeability and facilitating release of other mediators of inflammation (e.g. prostaglandins). In line with this finding, our data show an increase in *MMP-10* (4.5-fold), *MMP-1* (3.3-fold), *TRYPSIN-4* (sevenfold) (category 5, Table 1); these secreted factors are also potent promoters of tumor invasiveness and metastasis. In support of the notion that inflammation-related factors may be associated with cancer, inflammatory cells in conjunction with released metalloproteinases can promote tumor development, as shown by studies on skin tumorigenesis in mice lacking mast cells and *MMP-9* (Coussens *et al*., 1999). Collectively, there are compelling data suggesting a causal connection between inflammatory stimuli and cancer (reviewed in Coussens and Werb, 2002; Richmond, 2002). Finally, there is a striking downregulations of *PUMILIO-1* (−23-fold) and *p63* (−18-fold) transcripts upon UVB irradiation (category 9, Table 1); two developmental genes, believed to be required for the maintenance of stem cells *in vivo* and *in vitro* (see above refs and Wickens *et al*., 2002).

Cluster analysis

Clustering DNA chip data by means of the SPC algorithm (Blatt *et al*., 1996) is an unsupervised approach that aims at finding groups of genes with similar expression profiles (Kannan *et al*., 2001). Applying this method to the 573 genes identified in NHEK (Figure 4a) revealed a clear-cut partitioning/distinction between up- and downregulated ones (Figure 5a). We identified on the dendrogram six major stable clusters of genes: one large cluster (G6, of 153 genes) containing downregulated genes, and five that contain upregulated ones (clusters G1–G5, Figures 5a and b). Figure 5c shows the time courses of the average expression profiles of the genes in each of the clusters G1–G6, demonstrating their different patterns of gene activation. To visualize how certain genes that belong to a particular biological function are distributed among the clusters, we colored each cluster according to the proportion of genes belonging to functional category 6, which includes proinflammatory mediators (labeled '+', Table 1) and chemokines of the CXC/CC subfamilies. In addition, we marked the genes of category 6 by red crosses (Figure 5a). Six out of the 31 genes of cluster G2 are of category 6 ($\sim$20% purity), four of these (*IL-8*, *GRO-2*, *GRO-3*, and *SCYA20*) are members of the CXC/CC subfamilies ($\sim$30% efficiency of the CXC/CC subfamilies). Interestingly, among the genes that cluster together in G2, two are major transcription factors of *IL-8* (*JUNB* and *JUND*) (Table 1 and Figure 5a), and five are DNA repair-related genes (*GADD45A*, *TOB1*, *H2AA*, *H2BC*, *H2BQ*), suggesting that these functions may act in concert in the cellular response to UVB radiation.

Comparison of the transcriptional profiles of SCC and NHEK after UVB irradiation: CTWC analysis

Intersects of lists of genes, as visualized by Venn diagrams (Figure 4a), showed that 29 out of the 127 upregulated genes in SCC (23%) are common with NHEK, and 54 out of the 117 downregulated genes in SCC (46%) are in common with NHEK. This indicates high level of similarity in the response to UVB of both cell types, reflecting their common origin. However, although the transcriptional response of genes in NHEK and SCC appears complex in that many functional categories of genes contain both up- and downregulated genes (Tables 2 and 3), different patterns of activation and repression emerge for NHEK and SCC. In the transcriptional profile of genes involved in the regulation of apoptosis, *TNF*α, a major player in UVB-induced apoptosis, is more highly activated in SCC (>10-fold at two time points) than in NHEK (2.2-fold at one time point only, category 2, Table 1).

Table 1 Selected regulated genes in NHEK and SCC12B2 in response to UVB irradiation

			Normal keratinocytes (NHEK)					*SCC12B2*		
Symbol	*Name*	*Accession Nb.*		*0.5 h*	*3 h*	*6 h*	*12 h*	*24 h*		*6 h*	*12 h*
1 Cell cycle (+/−)/oncogene/tumor suppressor											
(+) CCNA1	Cyclin A1	U66838	↑	1.2	0.8	1.1	2.1	7.4		1.0	1.0
(+) CCNB1	Cyclin B1	M25753	↓	−1.1	−1.1	−1.4	−3.7	−4.3		−1.1	−1.7
(+) CCNB2	Cyclin B2	AL060146	↓	−1.6	−1.1	−1.3	−4.0	−4.3		−1.3	−1.6
(+) CCNE1	Cyclin E1	M74093	↓	−6.0	−1.7	−3.2	−7.2	−0.6		−1.7	−3.4
(+) ODC1	Ornithine Decarboxylase 1	M33764	↑	1.4	3.2	1.5	1.0	3.5		1.6	1.4
(+) HRAS	Ha-*ras* Oncogene	J00277	↑	6.9	1.3	2.3	1.7	2.6		−1.3	−1.7
*(+) MDM2	MDM2	M92424		0.9	0.9	1.5	1.9	1.1		1.0	1.0
(+/−) SFN	14-3-3 σ (Stratifin)	X57348	↑	1.4	1.5	2.2	2.0	1.1		−1.1	−1.1
(+) FYN	FYN oncogene	M14333	↓	−1.1	−1.3	−1.4	−4.9	−10.6		−1.8	−1.8
(+) ABL1	c-*abl* oncogene	X16416	↓	9.9	−1.4	−2.8	−3.8	−8.1		−2.2	−3.0
(+) ERBB3	c-*erb*-b2 Oncogene 3	M34309	↓	−1.8	−1.5	−3.2	−3.4	−1.1		−1.6	−1.6
(+) BCAR3	Breast Cancer Anti-Estrogen Resistance 3	U92715	↓	−1.0	−2.4	−3.1	−12.1	−3.9		−2.6	−5.8
(+) MK167	Antigen Ki-67	X65S50	↓	−1.0	−1.3	−1.2	−2.9	−5.2		−2.3	−2.2
(+) CSF2	CSF2	M13207		−1.1	−1.1	−1.1	−1.1	−1.1	↑	4.6	4.7
(−) PPP1R15A	GADD34	U63981	↑	9.8	1.0	1.4	2.2	5.1		−1.3	−1.1
*(−) CDKN1A	P21 CIP1	U03106		1.6	1.6	1.3	1.4	5.0		1.1	−1.2
(−) CDKN1C	P57 Kip2	064137	↑	1.6	2.0	2.2	1.3	3.5	↑	3.0	3.3
(−) CDKN1B	P27 Kip1	A1304854	↓	−1.7	−3.0	−1.4	−1.3	−3.4		1.0	1.0
(−) WEE1	WEE1	X62048	↓	−1.6	−6.7	−14.9	−18.9	−4.5	↓	−8.6	−0.8
*(−) TP53	P53 tumor suppressor	X02469		0.7	0.9	0.8	1.4	0.8		1.0	1.0
(−) NF2	Neurofibromatosis 2 tumor suppressor	AF122827	↑	1.0	1.8	6.9	10.0	1.4	↑	3.9	2.7
(−) FUS1	FUS1 tumor suppressor	AF055479		−1.1	−2.5	−2.7	−3.2	−1.7	↓	−3.9	−3.6
(−) FAT2	FAT2 tumor suppressor	ABO11535	↓	−1.3	−1.6	−3.6	−3.7	−7.9			
2 Apoptosis (+/−)											
(+) CRADD	RAIDD	U79115	↑	0.7	1.7	1.5	3.1	2.4		1.1	1.3
(+) TSSC3	Tumor suppressing STF 3	AF035444	↑	1.5	4.1	3.4	4.1	4.4		1.5	1.4
(+) PMAIP1	APR (NOXA)	090070	↑	2.0	7.0	14.7	16.1	13.0	↑	2.8	3.3
(+) TNF	TNFα	X02910		1.5	1.4	1.8	2.2	1.4	↑	10.5	10.4
(−) BCL2	BCL-2	H14745	↑	2.0	1.0	1.0	3.6	1.0		1.0	1.0
(−) API5L1	Antiapoptosis 5-Like 1	Y15906	↑	1.5	4.0	3.2	1.1	2.4		−1.1	−2.5
(−) IER3	Radiation-inducible IER3	SB1914	↑	1.5	5.2	5.1	5.4	4.5		1.4	1.2
(−) TNFAIP3	TNFα-Induced Protein 3	M59465	↑	1.0	0.7	1.2	2.4	6.8	↓	−3.7	−4.3
(−) HSPA2	HSP70	L26336	↑	1.8	1.0	2.1	2.2	1.9		1.0	1.0
(−) HSPCB	HSP90	W28616	↑	1.2	1.2	2.1	2.1	0.6	↑	2.3	2.8
(−) MCL1	Myeloid cell leukemia 1	L08246		0.8	0.4	0.4	0.4	1.6	↓	−7.4	−8.9
(−) BAG5	BCL2-Associated Athanogene 5	AB020680		1.0	0.6	0.4	0.5	1.1	↓	−3.5	−5.7
3 DNA repair											
GADD45A	GADD45A	MG0974	↑	1.5	3.6	4.7	7.0	9.2	↑	2.0	2.4
GADD45B	GADD45B	AF078077	↑	1.6	2.3	2.2	2.8	4.8		1.2	1.5
ERCC1	ERCC1	Ml 31 94	↑	1.2	2.0	1.4	1.1	3.9		1.3	1.3
ERCC2	ERCC2	AA079018	↑	1.1	1.6	2.4	2.2	1.4		1.3	1.9
BTG1	B-cell Translocation Gene 1	X61123	↑	1.1	1.3	1.7	2.2	3.4		1.1	−1.8
TOB1	Transducer of ErbB-2. 1	D38305	↑	8.9	1.5	2.0	2.0	2.5	↑	2.9	3.2
4 Oxydative stress/ROS metabolism (+/−)											
(+) CYBA	Superoxide-Generating NADPH Oxidase	M21186	↑	1.3	1.0	1.7	2.5	2.8		−1.1	−1.3
(−) MT1G	Matallothionein 1G	J03910	↑	1.0	3.2	3.4	2.0	3.8		1.6	1.3
(−) MT2A	Matallothionein 2A	A1547258		2.3	0.7	0.8	1.9	0.6	↓	−4.4	−3.6
(−) PRDX3	Peroxiredoxin 3	D49396		0.7	0.9	0.8	0.9	0.7	↑	2.2	2.4
5 Extra cellular matrix/protease (+/−)											
*(+) MMP1	Collagenase	M13509		0.8	1.4	1.3	1.8	3.3		1.5	1.8
(+) MMP10	Stromelysin 2	X07820	↑	1.8	2.5	2.2	2.1	4.5		1.0	1.8
(+) PRSS4	Trypsin 4	X71345	↑	1.4	2.2	1.4	1.9	7.0		1.0	1.0
6 Growth factor/chemokine/cytokine/inflammation (+/−)											
(+) IL8	IL-8 (CXC)	M28130	↑	2.0	10.6	36.8	48.1	71.7	↑	12.5	11.9
(+) IL6	IL-6	X04430	↑	1.0	1.3	4.1	3.7	1 9	↑	4.3	4.0
(+) IL1B	IL-1B	X04500	↑	1.0	1.3	1.4	1.6	1.9	↑	2.9	2.3
(+) GRO1	Small Inducible Cytokine B1 (MGSA) (CXC)	X54489	↑	2.2	1.7	2.2	3.1	3.2	↑	2.9	2.0

(+) GRO2	Small Inducible Cytokine B2 (CXC)	M36820	↑	1.4	3.9	5.8	6.0	5.1	↑	11.6	8.9
(+) GRO3	Small Inducible Cytokine B3 (CXC)	M36821	↑	2.0	2.4	6.8	7.9	5.2	↑	10.3	8.9
(+) PPBP	Small Inducible Cytokine B7 (NAP-2) (CXC)	M54995	↑	0.3	1.2	2.2	2.6	2.3		1.0	1.0
(+) SCYA20	Small Inducible Cytokine A20 (CC)	U64197	↑	1.9	3.7	11.5	21.5	17.0	↑	3.5	4.0
(+) PTGS2	Cyclooxygenase (COX-2)	U04636	↑	6.8	2.8	4.8	13.5	24.7	↑	5.5	7.8
(+) HB-EGF	HB-EGF-Like	M60278	↑	1.7	1.5	3.2	4.6	9.9		1.3	7.9
(+) S100A9	Calgranulin B	W72424	↑	1.1	1.5	1.6	2.2	6.0		1.3	1.7
INSL4	Insulin-like 4 (IGF family)	L34838	↑	1.0	12.0	13.4	20.2	26.1		−1.1	1.9
CTGF	IGFBP8	X78947	↑	1.3	3.8	5.6	6.3	1.3		1.1	1.1
CYR61	IGFBP10	Y11307	↑	1.3	2.8	3.4	2.4	3.6	↓	−9.8	−6.5
9 Development/differentiation (+/−)											
(+) TP63	p63(ΔNp63)	Y16961	↓	−0.9	−1.0	−2.0	−3.7	−16.0	↓	−2.4	−4.3
(+) PUM1	Pumilio 1	D43951	↓	−1.6	−3.2	−6.6	−23.7	−2.4	↓	−6.0	−10.3
(+) PUM2	Pumilio 2	D87078	↓	−1.3	−2.1	−3.1	−5.7	−2.8		−1.8	−2.5
11 Transcription (+/−)/replication											
(+) FOS	FOS	V01512	↑	5.4	4.7	4.7	2.1	0.6	↑	16.1	27.6
(+) JUN	JUN	J04111	↑	2.9	7.9	5.7	2.9	1.1		1.2	−1.1
(+) JUNB	JUNB	M29039	↑	2.0	4.5	3.6	4.0	3.4		1.3	−1.4
(+) JUND	JUND	X56681	↑	1.3	2.2	3.7	3.0	2.6	↑	3.7	2.0
(+) TLS/CHOP	GADD153	AA633221	↑	2.5	3.8	1.6	0.2	1.1		1.6	1.0
(+) MYC	MYC	V00568	↓	−1.5	−3.5	−3.2	−4.9	−4.2	↓	−6.9	−5.6
(+) E2F3	E2F3	D38550	↓	−1.4	−2.0	−3.6	−3.5	−2.9	↓	−3.3	−3.3
(+) E2F5	E2F5	U31556	↓	−1.2	−1.6	−1.3	−3.2	−6.3		−1.2	−1.1
*(+) RELA	NFkB (p65 subunit)	L19067		1.3	1.4	1.6	1.3	1.4		−1.3	−1.4
(−) TSC22	TGF β-Stimulated Protein	AJ222700	↑	1.2	2.3	4.0	3.1	1.6		−1.1	−1.5
(−) DRAP1	DR1-Associated Protein 1	U41843	↑	1.3	1.7	4.2	0.7	5.3	↑	2.6	3.7
(−) ATF3	ATF3	L19871	↑	1.3	3.8	4.7	10.8	17.1	↑	2.4	5.6
(−) ATF4	ATF4	AL022312	↑	1.2	1.7	2.1	2.2	3.1		1.2	1.0
(−) SAP18	Sin3-associated Polypeptide	W27641	↑	1.8	1.5	2.1	2.1	0.8		1.3	1.6
(−) ID2	Inhibitor of DNA Binding 2	D13891	↑	1.9	6.0	3.8	2.1	2.1	↑	14.6	22.0
12 Histone/chromatin											
H1FX	Histone H1X	D64142	↑	0.8	1.4	3.5	3.5	4.5		1.0	−1.1
H2AFA	Histone H2A A	AI039144	↑	1.1	4.6	9.4	13.4	12.4		1.0	1.0
H2AFG	Histone H2A G	ZB0776	↑	2.4	1.8	1.8	4.3	6.3		3.9	1.3
H2AFO	Histone H2A O	L19779	↑	1.5	3.2	2.1	3.0	18.0		1.9	2.0
H2AFX	Histone H2A X	XI4850	↑	1.0	2.5	0.7	1.3	3.2		1.2	1.0
H2BFA	Histone H2B A	AJ223352		1.1	0.9	1.2	1.1	2.4	↑	3.0	2.9
H2BFC	Histone H2B C	AL009179	↑	1.0	2.2	3.2	6.5	5.5		1.0	1.0
H2BFG	Histone H2B G	Z80779	↑	1.6	5.3	5.3	7.1	12.1		1.6	2.1
H2BFQ	Histone H2B Q	X57985	↑							1.1	1.3
MORF	Histone Acetyltransferase	AB002381	↓	−0.9	−1.4	−1.4	−5.4	−6.7		−2.6	−1.7
BAZ1A	Br Domain adj. to ZF1A (hist acetyltransferase)	AL050089	↓	−1.3	−1.9	−2.0	−3.9	−5.1		−1.1	−1.6
BAZ1B	Br Domain adj. to ZF1B (hist acetyltransferase)	AF072810	↓	−0.8	−1.1	−5.5	−3.4	−2.5		−1.7	−2.8

All genes that changed expression and passed the filtering threshold (see Figure 4) were classified into 14 functional categories as listed in Figure 6 and given in supplemental data in Tables 2 and 3. The list in Table 1 was selected from 9 categories of these lists (not including categories 7, 8, 10, 13 and 14) and illustrates the major changes in gene expression. Numbers show fold change of expression. Symbols '+' or '−' stand for positive or negative functional regulators, and '↑', or '↓' for UVB-induced up- or downregulation, respectively. The symbol '*' stands for six genes that are at the margin of the filtering threshold, but discussed in the Results and discussion section. Online Supplemental Data: Tables 2 and 3 containing full lists of up- and downregulated genes are available at http://www.weizmann.ac.il/~ligivol/

Furthermore, most of the antiapoptotic genes found upregulated in NHEK (*BCL-2* (3.6-fold), *API5L1* (4.0-fold), *IER3* (5.4-fold), *TNFAIP3* (6.8-fold) category 2, Table 1), are not regulated or are downregulated in SCC (category 2, Table 1), and the antiapoptotic genes *MCL1* and *BAG5* are found downregulated in SCC cells only (−8.9- and −5.7-fold, respectively, category 2, Table 1). Furthermore, in the variety of cytokines and growth factors induced in normal cells upon UVB irradiation, little or no induction of these genes is observed in SCC (category 6, Table 1). The relatively limited inflammatory response and induction of ECM proteases in SCC (categories 6 and 5, Table 1) as compared to NHEK may reflect their transformed state. Finally, in contrast to NHEK, DNA repair-related proteins are induced to a much smaller extent in SCC cells after UVB (categories 3 and 12, Table 1), suggesting some deficiency in the DNA repair machinery in these cells, and consequently that SCC are more prone to accumulation of mutations.

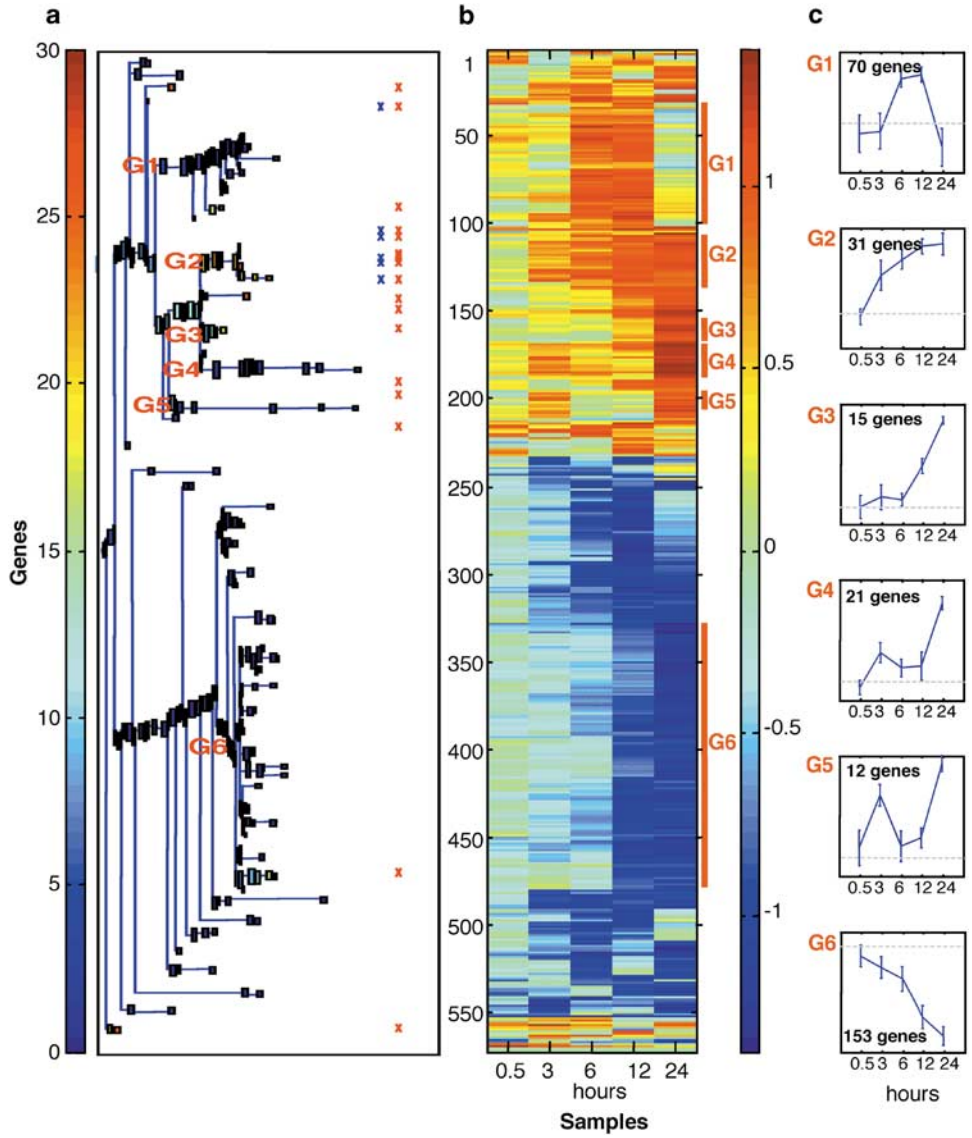

Figure 5 Clustering results of the 573 UVB-regulated genes in NHEK using the *super paramagnetic clustering* (SPC) algorithm. (**a**) Dendrogram showing clusters of genes with four or more members. Six stable clusters of genes (G1–G6) could be identified. Each cluster is represented by a box colored according to the proportion (left colorbar) of genes belonging to functional category 6 (Tables 1 and 2, 'cytokines and growth factors'). The distribution of these cytokines and growth factors genes (cluster G2 and red crosses), and that of chemokine genes of the CXC/CC subfamilies (blue crosses) is shown at the right. (**b**) Expression matrix of the up-(red) and down-(blue) UVB regulated genes (right colorbar). Centered and normalized $\log_2$ signals of the five time points post irradiation are shown (**c**). Average time course expression profiles of the genes in clusters G1–G6

Next, we used the unsupervised CTWC method to detect gene clusters, which distinguish best between NHEK and SCC samples or between before and after UVB irradiation samples. CTWC is an iterative unsupervised procedure, which uses the SPC method as its clustering engine and is designed to mine gene expression data. The algorithm identifies subsets of genes and samples such that when one of these is used to cluster the other, stable and significant partitions emerge. The method allows for the detection of small subsets of genes that partition between the samples and thereby identifies small number of key genes which may play a role in a particular biological process. This procedure avoids the 'noise' introduced by other genes which may mask the signal of the important players (Getz *et al*., 2000). We first selected from the combined NHEK and SCC data set 1269 genes (see the Materials and methods section). The first iteration of CTWC, denoted G1(S1), clustered all these genes on the basis of all samples, and this operation identified 33 stable gene clusters. Here, we focused on four of these gene clusters showing the most interesting and significant partitions of samples (Figure 6).

Cluster G24 contains 31 genes (Figure 6d) that separate the SCC from NHEK, since their expression levels are moderate in NHEK, but increase after UVB irradiation. In contrast, in SCC these genes remained low and nonresponsive to UVB. Of note, this cluster includes *S100A9*, *IL-IR L1*, *TRYPSIN-4*, and *MUCIN-1* (Figure 6), the latter being a notable tumor-associated antigen in breast cancer, and believed to play a role in tumor progression and metastasis (Xing *et al*., 2001).

Cluster G18 contains five genes (Figure 6a) that are UVB-downregulated in NHEK, whereas in SCC they exhibit constitutive high expression and are nonresponsive to UVB. Of note, this gene cluster contains two proapoptotic genes: *PARP* (Chiarugi and Moskowitz, 2002) and the cellular apoptosis susceptibility gene (*CAS*)(Brinkmann *et al*., 1996), supporting our biological observations that SCC are more sensitive to apoptosis.

Cluster G21 contains seven genes (Figure 6b) that show low expression levels in SCC and are nonresponsive to UVB exposure. In contrast, they show a moderate to high induction in NHEK in response to UVB. This cluster contains the metalloproteinases *MMP1* and *MMP10* that mediate tumor invasiveness, enable vascular permeability, and facilitate the release of other mediators of inflammation (Singh *et al*., 1999).

Cluster G28 contains 22 genes (Figure 6c) that are constitutively expressed at low levels in both SCC and NHEK before UVB, but are differentially upregulated after UVB exposure. Overall, this gene cluster is rich in genes of category 6, and to a lesser extent, in DNA repair-related genes (categories 3 and 12, Figure 6c). UVB exposure revealed for a number of genes of this

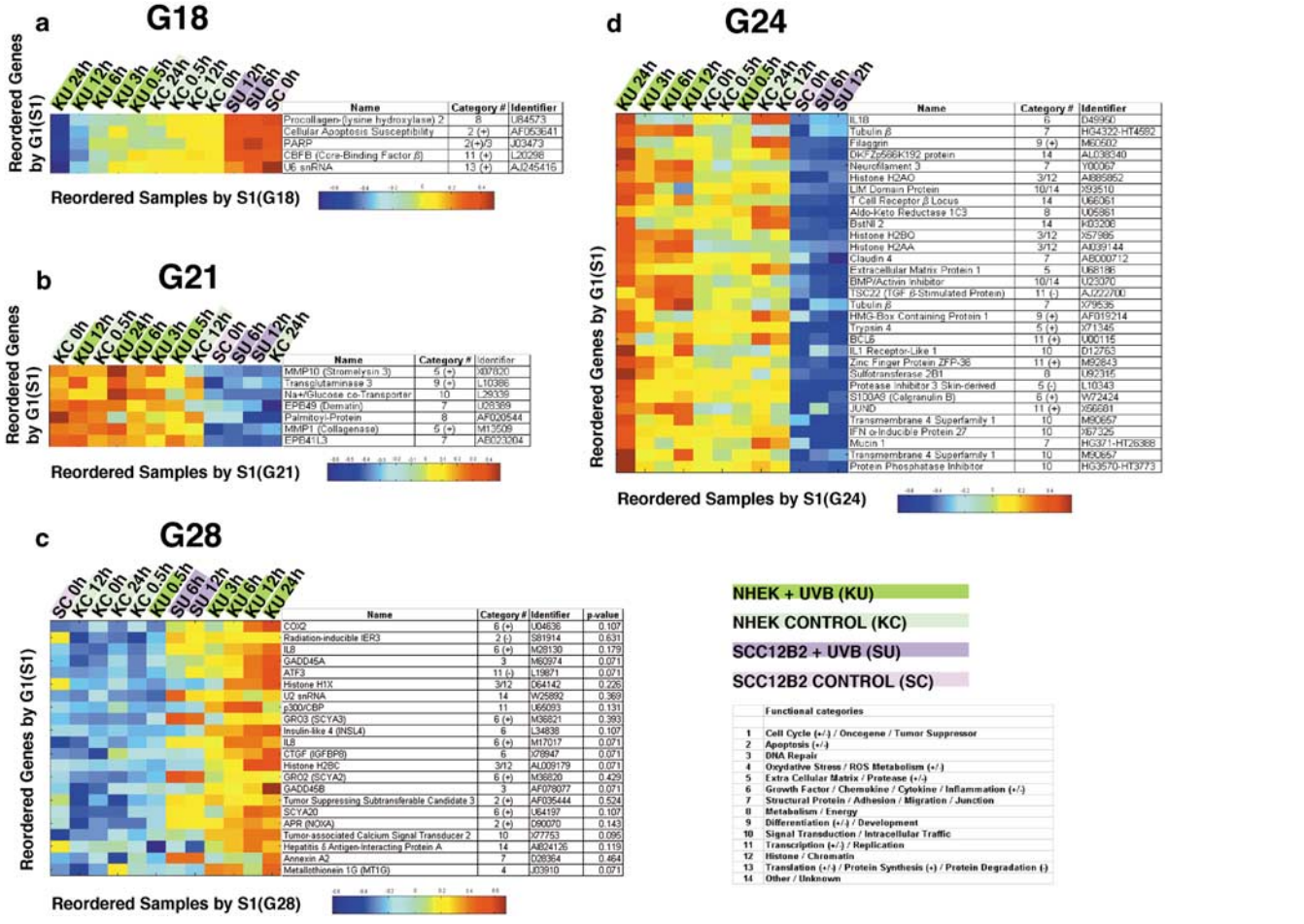

Figure 6 *Coupled two-way clustering* (CTWC) results showing partitions of genes and samples between NHEK and SCC. Each stable cluster identified by the CTWC method contains genes and samples reordered in an unsupervised coupled two way manner. Circled genes are discussed in the 'Results and discussion' section. (**a**) Genes downregulated in NHEK, but showing high expression and no response to UVB in SCC. (**b**) Genes that are UVB-responsive in normal keratinocyte cells only. (**c**) Genes that are upregulated in both cell types in response to UVB. *P*-values of the statistical significance associated to each gene were determined by comparing, in a permutation test, the expression levels following irradiation in NHEK versus SCC (genes highlighted in different colors according to their statistical significance). (**d**) Genes with low expression and no response to UVB in SCC, but high expression and moderate response to UVB in NHEK

category a significant difference in gene expression profile between NHEK and SCC. This holds in particular for *GADD45B*, the histone *H2BC*, the CC chemokine *SCYA20*, the growth factor *insulin-like-4* (*INSL4*), and the gene coding for the *Interacting Protein A of the Hepatitis δ Antigen* (*DIPA*) (Figure 6c).

Conclusion and significance

In summary, the transcriptional program of normal keratinocyte cells after intermediate UVB doses involves (i) expression of immediate-early transcription factors of the stress response, (ii) transcriptional activation of genes, which are characteristic of an inflammatory response, (iii) maintenance of cell proliferation, (iv) activation of the DNA repair genes, and (v) expression of cell survival factors. The reduction in apoptosis in a DNA damaging context may potentially lead to undesirable effect by increasing the number of living/surviving cells bearing DNA damage and mutations, which may later on become transformed (Green and Evan, 2002; Ziegler *et al*., 1994). The scheme shown in Figure 7 summarizes this information.

The CTWC method identified four stable clusters of genes that partitioned/separated normal keratinocytes (NHEK) from their tumor counterparts (SCC). These genes may be related to the carcinogenic pathway of SCC. Of note, the exposure to UVB resulted in different changes in gene expression in the two cell types, whereas their constitutive expression patterns were similar before UVB. This allowed us to identify discriminating genes that could otherwise not be revealed by simple comparison between normal and tumor samples in the absence of UVB irradiation (e.g. genes of cluster G28, where higher upregulation in NHEK is noticed). These differences in the response to UVB suggest their main cause stems from the transcription activation of these genes. We favor the possibility that tumorigenesis of SCC includes significant epigenetic effects that may be because of modifications (e.g. methylation) of promoter regions. In support of this possibility, several examples of gene inactivation in cancer were shown to be because of promoter methylation (e.g. *APAF-1*, *p16^{Ink4a}*, *COX-2*, *Fas*), which is extremely effective in maintaining the cancerous state.

The response of keratinocytes to the carcinogenic effect of UVB may explain the development of skin carcinoma. Furthermore, some of the genes involved, for example, *IL-8*, *GRO-1*, *GRO-3*, *COX-2*, and *MMPs* were found to be upregulated and to promote tumor growth, metastasis, and angiogenesis also in colorectal carcinomas (our unpublished data and Buckman *et al*., 1998; Loukinova *et al*., 2001; Notterman *et al*., 2001), and recent reviews emphasized the importance of *COX-2* as a potential target for colorectal cancer prevention (Gupta and Dubois, 2001; Turini and DuBois, 2002). Hence, the analysis of the effect of UVB on keratinocytes may serve as a model for the development of epithelial cancer in general.

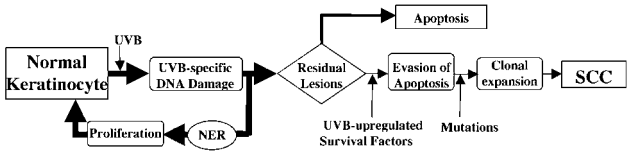

Figure 7 Model for the UV-induction of SCC. Schematic representation of the major pathways leading to SCC in response to UV irradiation

Materials and methods

Isolation of NHEK and cell cultures

Establishment of primary cultures and cell maintenance was performed as previously described (Dazard *et al*., 2000). Keratinocytes were freshly isolated from neonatal foreskin specimens derived from a normal human Caucasian. To allow proliferation without favoring differentiation, passages 2–3 of NHEK were maintained in FAD medium supplemented with 10% fetal bovine serum (FBS) and cocultured in the presence of mitomycin C-treated-feeder cells originating from the mouse fibroblast J2-3T3 cell line. The p53-mutant SCC12B2 cell line is derived from a human facial SCC, and the HaCaT cell line originates from a spontaneous immortalization of a human keratinocyte culture. All the cell lines were maintained in DMEM, supplemented with 10% FBS, except for the J2-3T3 cell line that was grown with 10% donor calf serum (DCS). Cell viability was determined by the trypan-blue exclusion test. Cell culture images were obtained on an ECLIPSE TE200 inverted microscope (NIKON®) equipped with a $\times 20$ objective and a COOLPIX 990 digital camera (NIKON®) interfaced to a PC computer. Images were further processed using AdobePhotoshop® software. Conditioned media were collected from cell cultures 48 h postirradiation and stored at -80°C until use. Media were added to the target cells immediately after UVB irradiation and renewed every 6 h for 48 h following irradiation.

Flow cytometry

Floating cells were collected and pooled with trypsinized cells. Fixation and staining were performed as previously described (Dazard *et al*., 2000). All cells were resuspended and filtered through a 70 μm mesh prior to analysis by flow cytometry on a Becton Dickinson FACScan®. For each sample, 10 000 events were gated and acquired in list mode.

UVB irradiation

UVB irradiation was performed on 80–90% confluent cultures. Cells were rinsed twice with prewarmed PBS at 37°C, then directly irradiated under a thin film of PBS$^-$ to avoid drying of cultures; the cells' own medium was restored after irradiation. The UVB source was a TFX-20 M, 6×15 W fluorescent lamp (Vilbert Lourmat, France) with an emission peak at 312 nm. The UV wavelengths shorter than 290 nm (UVC) were eliminated using a cellulose acetate cutoff filter (Kodacel®, Kodak, France). The UVB flux, measured by means of a dosimeter (HD9021, Delta Ohm, Italy), was 0.312 mW/cm^2 at 19 cm from the source. Cells were either subjected to a single UVB exposure at doses ranging from 200 to 800 J/m^2, or to multiple daily doses of 200 J/m^2 for three (SCC12B2) or five (NHEK) consecutive days. Assays were performed at the indicated times following irradiation.

TNFα-induced apoptosis

Confluent HaCaT cultures were treated with TNFα (20 ng/ml) combined with actinomycin D (2 μg/ml) (Sigma, St Louis, MO, USA) for 12 h, after which time, adherent and floating cells were pooled and lysed for total protein extraction.

Antibodies and immunoblot analysis

For immunoblot detection, the following Abs were used: a mixture of monoclonal p53 Abs DO1 and 1801 (gift of M Oren); a mixture of monoclonal MDM2 Abs 4B2 and 2A9 (gift of M Oren); monoclonal p63 Ab 4A4; polyclonal $p21^{Cip1}$ Ab C19 (Santa Cruz Biotechnology, CA, USA); polyclonal $p16^{Ink4a}$ Ab C20 (Santa Cruz Biotechnology, CA, USA); monoclonal GAPDH Ab MAB374 (CHEMICON, Temecula, CA, USA); polyclonal PARP Ab (gift of G de Murcia); polyclonal caspase-3 Ab H277 (Santa Cruz Biotechnology, CA, USA); monoclonal caspase-8 Ab 1C12 (Cell Signaling, Beverly, MA, USA); monoclonal caspase-9 Ab 96-2-22 (Upstate Biotechnology, Lake Placid, NY, USA); monoclonal involucrin Ab SY5 (Novocastra, Newcastle, England); polyclonal cornifin Ab (gift of A Jetten). Total cell lysates, protein resolution by PAGE, transfer on nitrocellulose membrane (Bio-Rad), and immunoblotting were performed as previously described (Dazard *et al*., 2000). Detection was performed using the Western blotting-enhanced chemiluminescence substrate (ECL + plus, Amersham Pharmacia Biotech, Buckinghamshire, England) following the supplier's protocol.

RNA extraction, microarray hybridization and analysis

RNA was extracted by standard methods. Cells were lysed directly in their Petri dishes in TRIzol reagent (Gibco Invitrogen, Carlsbad, CA, USA) and total RNA was isolated according to the manufacturer's instructions. cRNA preparation and microarray hybridization were carried out according to the supplier (Affymetrix®, Santa Clara, CA, USA), using Genechip® HG-U95Av2. Scanned output files were analysed by the probe level analysis package, Microarray Suite MAS 5.0 (Affymetrix®, Santa Clara, CA, USA). Only genes that were 'Present' in the 'Present/Absent' call provided by the Affymetrix® program in at least one time point were selected and further referred to as 'legal' (i.e. significantly expressed). 5818 'legal' genes were selected for further analyses. The signal for each of these genes was determined from the 'probeset' in use for this gene and by the probe level analysis method provided by the Affymetrix® software; if lower than 30, it was adjusted to 30. The control for NHEK was the average of the four control time points (0, 0.5, 12, and 24 h). Genes were classified into 14 functional categories according to the annotations provided by the Gene Ontology™ consortium (http://www.godatabase.org/cgi-bin/go.cgi) and GeneCards™ database (http://bioinformatics.weizmann.ac.il/cards/).

Super-paramagnetic clustering analysis

Clustering analysis was carried out using the unsupervised *Super paramagnetic clustering* (SPC) algorithm (Blatt *et al*., 1996). The selected data set consisted of up- and down-regulated genes that met our criteria for change of expression, at six experimental time points (0, 0.5, 3, 6, 12, and 24 h). The resulting data set is an expression matrix A in which each row i ($i = 1, 2, \ldots, 573$) represents a gene vector, each column j ($j = 1,\ldots,6$), a time point over the time course experiment (sample vector) and where each element A_{ij} of A, is the $\log_2$ transformed signal of the gene i, measured at time point j. Before clustering, each gene vector was centered and normalized, such that the mean of its components was set to 0, and the sum of squares to 1. The resulting expression matrix was denoted B. Next, from each component C_{ij} of the reordered expression matrix, denoted C after clustering, the first component C_{ij} was subtracted, such that each gene vector starts with a zero value in its first component, corresponding to time point 0 h. The 0 h column was then removed (Figure 5b).

The clustering algorithm measures the distance between the genes, using the regular Euclidean distance between their normalized values. Genes with similar time course expression profiles are represented by two nearby vectors and are placed in the same cluster. Stable clusters are defined and identified as described elsewhere (http://ctwc.weizmann.ac.il/stable_clusters.html). The properties of 'purity' and 'efficiency', used further in gene cluster analysis, refer to the fraction of genes of this cluster, which belong to a given group of interest, and to the fraction of genes of the given group, which belong to the considered cluster.

CTWC analysis

CTWC (Getz *et al*., 2000; http://ctwc.weizmann.ac.il/ctwc.html) analysis was performed on the DNA chip data sets taken from all samples of both NHEK and SCC gene expression experiments. Data sets were merged to generate a complete gene expression matrix. Values less than 30 were rescaled to 30 and $\log_2$ transformed. Only genes with a standard deviation (of the transformed data) greater than one were selected, and then centered and normalized as described above. This yielded an expression matrix of 1269 genes by 12 samples. As for the choice of the optimal K-nearest neighbors parameter for the clustering algorithm, default parameters for the genes ($K = 12$) and for the samples ($K = 4$) were chosen. The data were first clustered in two ways; the first operation, denoted G1(S1), clustered all the genes on the basis of their expression levels over all S1 samples. The complementary operation, denoted S1(G1), clusters all the samples on the basis of their expression levels over all G1 genes. The method identifies all stable clusters of either genes (or samples). It then scans through all stable clusters of genes (or samples), one by one and uses each of them to cluster all the S1 samples (or G1 genes) and thereby to identify stable clusters of samples (or genes).

Abbreviations

NHEK, normal human epidermal keratinocyte; SCC, squamous cell carcinoma; UVB, ultraviolet B; NER, nucleotide excision repair; CTWC, coupled two-way clustering; SPC, super paramagnetic clustering

Acknowledgements

We are grateful to the family of Arison Dorsman for their donation to the Center for DNA Chips in the Pediatric Oncology Department, The Chaim Sheba Medical Center, Tel-Aviv. This study was supported in part by the Yad Abraham Research Center for Cancer Diagnosis and Therapy, and grants from the Irwin Green Alzheimer's Research Fund, the Israel Science Foundation (ISF) and the Germany–Israel Science Foundation (GIF). We thank M Oren for monoclonal antibodies against p53 and MDM2, A Jetten for the polyclonal antibody against Cornifin, G de Murcia for the polyclonal antibody against PARP, and N Fusenig for HaCaT cells.

References

Ahmad N, Gilliam AC, Katiyar SK, O'Brien TG and Mukhtar H. (2001). *Am. J. Pathol.,* **159,** 885–892.

Armstrong BK and Kricker A. (2001). *J. Photochem. Photobiol. B,* **63,** 8–18.

Bassing CH, Chua KF, Sekiguchi J, Suh H, Whitlow SR, Fleming JC, Monroe BC, Ciccone DN, Yan C, Vlasakova, Livingston DM, Ferguson DO, Scully R and Alt FW. (2002). *Proc. Natl. Acad. Sci. USA,* **99,** 8173–8178.

Blatt M, Wiseman S and Domany E. (1996). *Phys. Rev. Lett.,* **76,** 3251–3254.

Brash DE. (1997). *Trends Genet.,* **13,** 410–414.

Brinkmann U, Brinkmann E, Gallo M, Scherf U and Pastan I. (1996). *Biochemistry,* **35,** 6891–6899.

Brune B and von Knethen A. (2002). *J. Environ. Pathol. Toxicol. Oncol.,* **21,** 103–112.

Buckman SY, Gresham A, Hale P, Hruza G, Anast J, Masferrer J and Pentland AP. (1998). *Carcinogenesis,* **19,** 723–729.

Burns JE, Baird MC, Clark LJ, Burns PA, Edington K, Chapman C, Mitchell R, Robertson G, Soutar D and Parkinson EK. (1993). *Br. J. Cancer,* **67,** 1274–1284.

Celeste A, Petersen S, Romanienko PJ, Fernandez-Capetillo O, Chen HT, Sedelnikova OA, Reina-San-Martin B, Coppola V, Meffre E, Difilippantonio MJ, Redon C, Pilch DR, Olaru A, Eckhaus M, Camerini-Otero RD, Tessarollo L, Livak F, Manova K, Bonner WM, Nussenzweig MC and Nussenzweig A. (2002). *Science,* **296,** 922–927.

Chazal M, Marionnet C, Michel L, Mollier K, Dazard JE, Della Valle V, Larsen CJ, Gras MP and Basset-Seguin N. (2002). *Oncogene,* **21,** 2652–2661.

Chiarugi A and Moskowitz MA. (2002). *Science,* **297,** 200–201.

Chung HT, Pae HO, Choi BM, Billiar TR and Kim YM. (2001). *Biochem. Biophys. Res. Commun.,* **282,** 1075–1079.

Cleaver JE and Crowley E. (2002). *Front. Biosci.,* **7,** d1024–d1043.

Coussens LM, Raymond WW, Bergers G, Laig-Webster M, Behrendtsen O, Werb Z, Caughey GH and Hanahan D. (1999). *Genes Dev.,* **13,** 1382–1397.

Coussens LM and Werb Z. (2002). *Nature,* **420,** 860–867.

Dazard JE, Piette J, Basset-Seguin N, Blanchard JM and Gandarillas A. (2000). *Oncogene,* **19,** 3693–3705.

Decraene D, Agostinis P, Bouillon R, Degreef H and Garmyn M. (2002). *J. Biol. Chem.,* **277,** 32587–32595.

Evan GI and Vousden KH. (2001). *Nature,* **411,** 342–348.

Fang L, Li G, Liu G, Lee SW and Aaronson SA. (2001). *EMBO J.,* **20,** 1931–1939.

Garssen J and van Loveren H. (2001). *Crit. Rev. Immunol.,* **21,** 359–397.

Getz G, Levine E and Domany E. (2000). *Proc. Natl. Acad. Sci. USA,* **97,** 12079–12084.

Gloster Jr HM and Brodland DG. (1996). *Dermatol. Surg.,* **22,** 217–226.

Green DR and Evan GI. (2002). *Cancer Cell,* **1,** 19–30.

Greinert R, Boguhn O, Harder D, Breitbart EW, Mitchell DL and Volkmer B. (2000). *Photochem. Photobiol.,* **72,** 701–708.

Gupta RA and Dubois RN. (2001). *Nat. Rev. Cancer,* **1,** 11–21.

Han JA, Kim JI, Ongusaha PP, Hwang DH, Ballou LR, Mahale A, Aaronson SA and Lee SW. (2002). *EMBO J.,* **21,** 5635–5644.

Hanson KM and Clegg RM. (2002). *Photochem. Photobiol.,* **76,** 57–63.

Kannan K, Amariglio N, Rechavi G, Jakob-Hirsch J, Kela I, Kaminski N, Getz G, Domany E and Givol D. (2001). *Oncogene,* **20,** 2225–2234.

Karin M, Cao Y, Greten FR and Li ZW. (2002). *Nat. Rev. Cancer,* **2,** 301–310.

Li D, Turi TG, Schuck A, Freedberg IM, Khitrov G and Blumenberg M. (2001). *FASEB J.,* **15,** 2533–2535.

Liefer KM, Koster MI, Wang XJ, Yang A, McKeon F and Roop DR. (2000). *Cancer Res.,* **60,** 4016–4020.

Lotem J, Kama R and Sachs L. (1999). *Proc. Natl. Acad. Sci. USA,* **96,** 12016–12020.

Loukinova E, Chen Z, Van Waes C and Dong G. (2001). *Int. J. Cancer,* **94,** 637–644.

Martini EM, Keeney S and Osley MA. (2002). *Genetics,* **160,** 1375–1387.

Michael D and Oren M. (2002). *Curr. Opin. Genet. Dev.,* **12,** 53–59.

Notterman DA, Alon U, Sierk AJ and Levine AJ. (2001). *Cancer Res.,* **61,** 3124–3130.

Parsa R, Yang A, McKeon F and Green H. (1999). *J. Invest. Dermatol.,* **113,** 1099–1105.

Pellegrini G, Dellambra E, Golisano O, Martinelli E, Fantozzi I, Bondanza S, Ponzin D, McKeon F and De Luca M. (2001). *Proc. Natl. Acad. Sci. USA,* **98,** 3156–3161.

Pfeiffer GP. (1997). *Photochem. and Photobiol.,* **65,** 270–283.

Richmond A. (2002). *Nat. Rev. Immunol.,* **2,** 664–674.

Sage E, Lamolet B, Brulay E, Moustacchi E, Chteauneuf A and Drobetsky EA. (1996). *Proc. Natl. Acad. Sci. USA,* **93,** 176–180.

Selgrade MK, Smith MV, Oberhelman-Bragg LJ, LeVee GJ, Koren HS and Cooper KD. (2001). *Photochem. Photobiol.,* **74,** 88–95.

Sesto A, Navarro M, Burslem F and Jorcano JL. (2002). *Proc. Natl. Acad. Sci. USA,* **99,** 2965–2970.

Singh RK, Varney ML, Bucana CD and Johansson SL. (1999). *Melanoma Res.,* **9,** 383–387.

Soehnge H, Ouhtit A and Ananthaswamy ON. (1997). *Front. Biosci.,* **2,** D538–D551.

Soufir N, Moles JP, Vilmer C, Moch C, Verola O, Rivet J, Tesniere A, Dubertret L and Basset-Seguin N. (1999). *Oncogene,* **18,** 5477–5481.

Tsujii M and DuBois RN. (1995). *Cell,* **83,** 493–501.

Turini ME and DuBois RN. (2002). *Annu. Rev. Med.,* **53,** 35–57.

Wickens M, Bernstein DS, Kimble J and Parker R. (2002). *Trends Genet.,* **18,** 150–157.

Xie K. (2001). *Cytokine Growth Factor Rev.,* **12,** 375–391.

Xing PX, Apostolopoulos V, Pietersz G and McKenzie IF. (2001). *Front. Biosci.,* **6,** D1284–D1295.

Yang A, Kaghad M, Wang Y, Gillett E, Fleming MD, Dotsch V, Andrews NC, Caput D and McKeon F. (1998). *Mol. Cell,* 305–316.

Yang A, Schweitzer R, Sun D, Kaghad M, Walker N, Bronson RT, Tabin C, Sharpe A, Caput D, Crum C and McKeon I. (1999). *Nature,* **398,** 714–718.

Zhao R, Gish K, Murphy M, Yin Y, Notterman D, Hoffman WH, Tom E, Mack DH and Levine AJ. (2000). *Genes Dev.,* **1,** 981–993.

Ziegler A, Jonason AS, Leffell DJ, Simon JA, Sharma HW, Kimmelman J, Remington L, Jacks T and Brash DE. (1994). *Nature,* **372,** 773–776.